A&A 385, 986–994 (2002)
DOI: 10.1051/0004-6361:20020186

Astronomy & Astrophysics

FUSE observations towards the pole-on Be star HR 5223⋆

Y. Frémat[1], J. Zorec[2], A.-M. Hubert[1], L. S. Cidale[3], R. D. Rohrmann[4], J.-M. Désert[2], R. Ferlet[2],, and A. Vidal-Madjar[2]

[1] Observatoire de Paris, Section d'Astrophysique de Meudon, GEPI, FRE K 2459, 5 place Jules Janssen, 92195 Meudon Cedex, France
[2] Institut d'Astrophysique de Paris, CNRS, 98bis boulevard Arago, 75014 Paris, France
[3] Facultad de Ciencias Astronómicas y Geofisicas, Universidad Nacional de La Plata, Paseo del Bosque S/N, 1900 La Plata, Argentina
[4] Observatorio Astronómico, Universidad Nacional de Córdoba, Laprida 854, 5000 Córdoba, Argentina

Received 26 October, 2001 / Accepted 29 January 2002

Abstract. New spectra have been obtained for the pole-on Be star HR 5223 (HD 120991) using the Far Ultraviolet Satellite Explorer (FUSE). We give a complete description of the far-UV spectral range (920 to 1180 Å). The spectra are affected by strong blends with interstellar lines and molecular bands that also significantly lower the energy distribution of the star. We produce a synthetic spectrum of the interstellar medium (ISM) to determine the column densities of several elements (H_2, H I, N I, O I ...) seen towards HR 5223 and to disentangle the components due to the ISM, the photosphere and/or to the circumstellar envelope. The line identification list is available at the CDS. Using the obtained column densities, we determine the reddening of the star due to the ISM only and locate the star relative to the nearby IS clouds. The fit of the dereddened UV flux distribution with models that account for the gravitational darkening due to the stellar fast rotation allowed us to estimate the stellar fundamental parameters ($T_{\rm eff}$ = 22 000 K; log g = 3.7) and its distance ($d = 834 \pm 20$ pc). The distance obtained, which has to be considered as the most accurate available at the moment, is in agreement with the characteristics of the ISM matter distribution that affects the observed spectrum of the star and with the detecting limits of the HIPPARCOS satellite.

Key words. stars: emission-line, Be – stars: fundamental parameters – stars: individual: HR 5223 – stars: rotation – ISM: abundances – stars: distances

1. Introduction

It is commonly accepted that Be stars are non-supergiant stars showing – or having shown – one or more Balmer lines in emission (Jaschek et al. 1981). They represent 17% of the whole galactic B type stars population and are subject to fast rotation. Rotation not only affects stellar evolution, but it deforms also the photosphere and produces non-uniform surface gravity and temperature distributions. Consequently, all observable stellar parameters are dependent on the viewing angle i between the star's rotation axis and the line of sight. If we combine these effects with electron scattering, bound-free and free-free emission arising from the surrounding envelope, the interstellar extinction and the stellar fundamental parameters are very difficult to determine. This difficulty is furthermore increased by the fact that Be stars are generally far-away objects with very low angular diameters, so that the shape of the circumstellar envelope (CE, disk or ellipsoid) is still an actively debated subject. Remoteness implies also that their parallaxes, if known, are often inaccurate even when they are measured with the HIPPARCOS satellite. The distance knowledge is, however, very useful to determine the absolute radiation fluxes observed at the stellar surface in order to test the theoretically predicted fluxes.

In the present work, we are mainly dealing with the difficulties related to the fundamental parameter determination and the distance knowledge of the pole-on Be star HR 5223 recently observed by FUSE (Far Ultraviolet Satellite Explorer). The studied star is briefly described in Sect. 2. Interstellar lines appearing in the FUSE spectra (see Sect. 3) are first studied in order to evaluate their effect on the energy distribution and the stellar line profiles. The methods used to compute the synthetic spectra are fully explained in Sect. 4, while the derived column densities, the identification line lists and interstellar reddening for the star are given and discussed in Sect. 5. Using FUSE fluxes combined with IUE spectra, we determine in Sect. 6

Send offprint requests to: Y. Frémat,
e-mail: yves.fremat@obspm.fr
⋆ Table 2 is only available in electronic form at http://www.edpsciences.org

Table 1. Log of FUSE observations

Dataset Name	Date
Q1140101001	June 30, 2000
Q1140101002	June 30, 2000
Q1140101003	July 01, 2000
Q1140101004	July 01, 2000

the distance to HR 5223 and compare our value and its location relative to the local interstellar clouds. Conclusions are finally given in Sect. 7.

2. The star

The star (HR 5223 ≡ HD 120991 ≡ V767 Cen) was classified B2IIIe by Hiltner et al. (1969). All along its recorded lifetime, it showed strong and variable emission features. Fleming (1890) was the first to notice emission in the Hβ hydrogen line while Campbell (1895) observed a strong Hα emission line. Following Hanuschik (1996) and Hanuschik et al. (1996) the Fe II *class 2* emission line profiles are well defined, asymmetrical and double peaked. They also show a weak *V/R* variability (Hanuschik et al. 1995), while hydrogen emission lines exhibit strong line profile variations (Dachs et al. 1992). Modeling the winebottle structure observed in 1987 for the Hα emission line, Hummel (1994) deduced an inclination angle for HR 5223 of the order of 15 degrees. However, his model could not fit the broad wings of the line, which are probably due to non-coherent electron scattering. In this case, electron scattering should be an important opacity source in the star's circumstellar environment.

The IUE spectra, which are typically those of an early type-star have been studied by Dachs & Hanuschik (1984) for the first time. Most of the observed resonance lines are dominated by features arising from the interstellar medium and showing heliocentric radial velocities close to zero. The profiles of N V, C IV and Si IV UV resonance lines are slightly asymmetric but there is no clear evidence that these lines are formed in a high velocity expanding envelope (Hubeny et al. 1986). Following Hubeny et al. (1986), the studied ultraviolet spectra seem to correspond to the stellar photospheric spectrum. The fact that the UV energy distribution observed by IUE at different dates does not vary significantly tends to confirm this assertion.

3. FUSE observations (λλ 920–1180 Å)

The FUSE (Far Ultraviolet Spectroscopic Explorer) satellite and the on board spectrograph have been described by Moos et al. (2000) and Sahnow et al. (2000). The total exposure time for the observations, described in Table 1, was 518 s. They were performed with the large aperture (LWRS) in TTAG mode (photon mode). Data were extracted using the CALFUSE (Version 1.8.7) standard reduction pipeline which provided us with flux and wavelength calibrated spectra for the complete set of individual exposures. In order to increase the *S/N* ratio, the exposures from segments "a" and "b" of each channel (SiC1, SiC2, LiF1, LiF2) were co-added with the IAP XIPLOT IDL package.

Due to observational and satellite guiding errors, the wavelength scale was redshifted. This shift has been corrected using the line centers of several narrow molecular hydrogen lines. The absolute wavelength calibration was obtained by aligning the FUSE ISM absorption lines with those observed in the IUE spectra analyzed and discussed by Dachs & Hanuschik (1984). The final spectra were finally rebinned over 3 pixels. In this way, the mean spectral resolution we obtained is about 0.07 Å.

4. Theoretical spectra

The computed theoretical spectrum contains both photospheric and interstellar medium effects. In our approach, the interstellar (Sect. 4.3) and photospheric contribution (Sects. 4.1 and 4.2) are computed in two different, fairly independent, but consecutive steps of an iterative procedure, which allows us to determine both the ISM characteristics and the stellar fundamental parameters. In the first step, only the far-UV interstellar line profiles and bands are fitted. In the second step, we reproduce the FUSE and IUE spectral ranges of the observed star by multiplying the theoretical photospheric contribution by the normalized synthetic spectrum of the interstellar component calculated in the first step. The result thus obtained is then used to fit the observed energy distribution. It is the goodness of this fit that determines the final choice of the stellar fundamental parameters. In the next sections we deepen somewhat into details of each iteration step.

4.1. Photospheric spectrum

Stellar spectra were computed using Kurucz (1994) LTE model atmopheres and the SYNSPEC package (Hubeny 1988) available at the CCP7 database.

As stated in Sect. 2, the far-UV spectrum of HR 5223 observed by IUE reveals no variations while the star changes in the visible spectral range. Thus its fundamental parameters have been determined using the ultraviolet energy distribution between 920 and 3300 Å, which yields: $T_{\rm eff} = 22\,000$ K and $\log\ g = 3.70$. As this determination is closely related to the distance determination, we postpone the discussion of the method used to Sect. 6.1.

Differential Doppler broadening of line shapes due to stellar rotation has be accounted for with a projected rotational velocity $V \sin\ i = 70$ km s^{-1} (Slettebak 1982). The line list we used is the one of Kurucz updated by Hubeny and also available at the CCP7 ftp server.

4.2. Rapid rotation effects on the continuum

In order to account for the effects of rapid rotation on the continuum, we used the Roche approximation and the von Zeipel law which enabled us to compute, respectively, the local gravity and effective temperature distributions

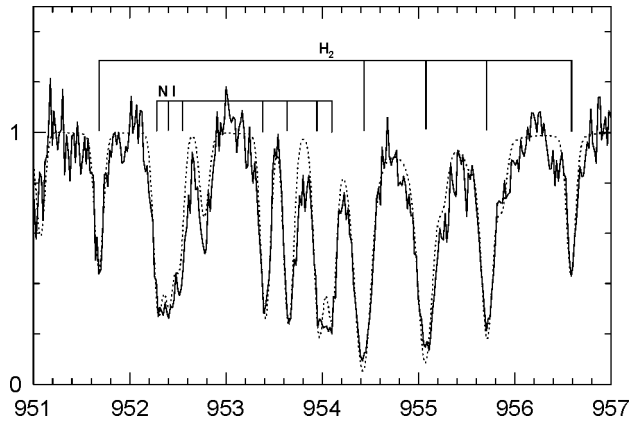

Fig. 1. Fit of the interstellar spectrum. The extracted interstellar spectrum (solid line) is compared to the fit results (dotted line).

on the stellar surface. Each local atmospheric structure has been described with Kurucz's LTE model atmospheres (1994).

4.3. Interstellar spectrum

As stated above, the spectral range covered by FUSE is dominated by blends with strong interstellar molecular bands (H_2, CO) and interstellar lines (H I, O I etc.). Identification of these blends have been carried out according to a line list updated from Morton (2001) and provided with the OWENS computer code developed by Lemoine et al. (1999).

The OWENS code was further used to fit the interstellar lines by a χ^2 minimization procedure allowing to adjust parameters such as the kinetic temperature, radial velocity, turbulence speed, column density (CD), background level and continuum shape. In order to avoid numerical instabilities, due to the complexity of the continuum fitting in the FUSE spectra and to the strong ISM line and bands blending, we divided the observed spectrum by a model photospheric spectrum; both spectra are normalized previously. The theoretical spectrum is only to give an approximate representation of the background radiation, which helps to draw the *pseudo* continuum underlying the observed ISM lines and bands. We note that the fit of the ISM lines and blends actually does not depend strongly on the precise choice of the fundamental parameters for the model continuum spectrum. In the end, the representation of the continuum is done using second order polynomials and the fit of the ISM lines and bands is sought so as to account simultaneously for the whole spectral range studied. In this fit we excluded the regions polluted by airglow emission (Feldman et al. 2001) and those exhibiting saturated absorption lines. This procedure (see Fig. 1 for an example of the results obtained) gave us a coherent set of CDs for all elements detected in the interstellar medium towards HR 5223.

As we fitted a large spectral range including gradually all the studied molecules and atoms, we think that the major uncertainty source affecting the column densities is related to the continuum fitting. The continuum is, indeed, not only perturbed by noise but also by the remaining effects due to the stellar spectrum. In order to estimate the error bars on the CDs given by our best fit, we used several intermediary results provided by the procedure we adopted. This allowed us to explore a set of column density values computed for a smaller spectral range but assuming polynomials of different orders (first, second and third order) to fit the continuum. The column density error bars were directly deduced from the variance of these intermediary results while the accuracy of the b factor adopted in Table 3 was derived from the largest deviation that occurred relative to its *best* value.

Table 3. Column Densities (CD) towards HR 5223.

Element	$\log N$ [cm^{-2}]	**b** [km s^{-1}]
H_2 ($J=0$)	18.84 ± 0.01	3.5 ± 0.3
H_2 ($J=1$)	18.91 ± 0.02	3.5
H_2 ($J=2$)	17.53 ± 0.12	3.5
H_2 ($J=3$)	17.23 ± 0.15	3.5
H_2 ($J=4$)	14.60 ± 0.11	3.5
H_2 ($J=5$)	$\leq$14.12	3.5
H I	20.49±0.15	6.0 ± 0.4
C I	≤ 13.47	6.0
N I	16.43 ± 0.21	6.0
O I	17.25 ± 0.15	6.0
Al II	≤ 16.69	6.0
Si II	15.85 ± 0.07	6.0
P II	13.89 ± 0.23	6.0
Cl I	≤ 12.74	6.0
Ar I	14.69 ± 0.21	6.0
Fe II	14.61 ± 0.09	6.0

5. Far-UV spectrum

The theoretical spectrum in the FUSE spectral range is compared to the observed one. Figure 2 shows the results obtained. In this figure the observed spectrum is represented by a solid line, the computed spectrum without IS lines is shown in dashed lines and the spectrum with IS lines is in a dotted line. For clarity purposes all these spectra were shifted.

The line identification list is given in Table 2 which is available at the CDS. In this table are given the observed wavelengths (Col. 1); the laboratory wavelengths (Col. 2) and the line identification (Col. 3).

5.1. Interstellar spectrum

231 transitions arising from the interstellar medium have been identified. Our best fit shows two ISM regions: a cold component where H_2 lines are formed with a total Doppler line width $b = 3.5$ km s^{-1}, and a second component where arise neutral and singly ionized lines (H I, Fe II etc.) with a Doppler line width of about 6 km s^{-1}. Heliocentric radial velocities of both components are close to 0 km s^{-1},

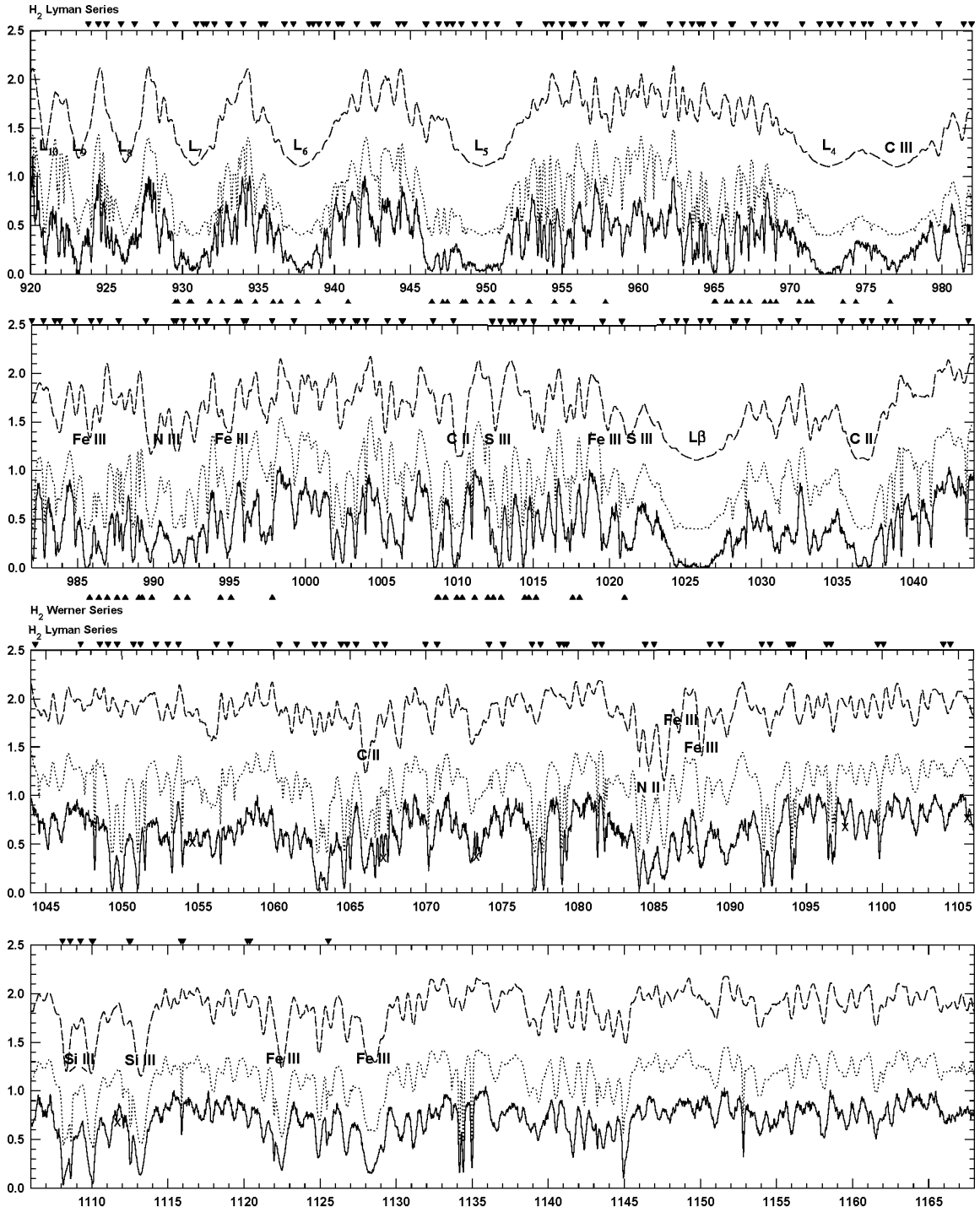

Fig. 2. Comparison between theoretical and observed spectra (full line). Theoretical spectra computed with (dotted line) and without (dashed lines) IS lines have been shifted vertically. Interstellar H_2 lines are identified by up (Werner Series) and down (Lyman Series) black triangles. Identified instrumental artifacts are cross marked while some stellar lines are identified. Solar chemical composition is assumed for the theoretical stellar spectrum.

if we refer to the IUE spectra as the absolute wavelength calibration (Dachs & Hanuschik 1984). The column densities (cm^{-2}) and Doppler widths (km s^{-1}) obtained in both regions are given for each ion or molecule in Col. 2 and 3 of Table 3, respectively. It is worth noting that our results do not depend very much on the background radiation (Sect. 4) considered during the fit. Neutral hydrogen was the most affected IS element with a maximum relative variation on its CD of about 8%. The expected uncertainty on the column densities given in Table 3 accounts for this effect.

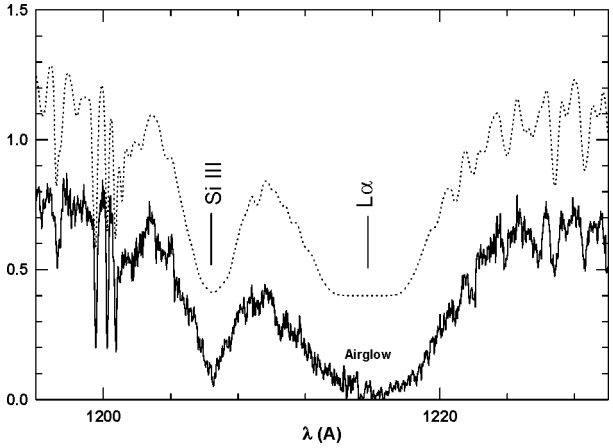

Fig. 3. Comparison between the observed (solid line) and theoretical (vertically shifted dotted line) Lα line-profile.

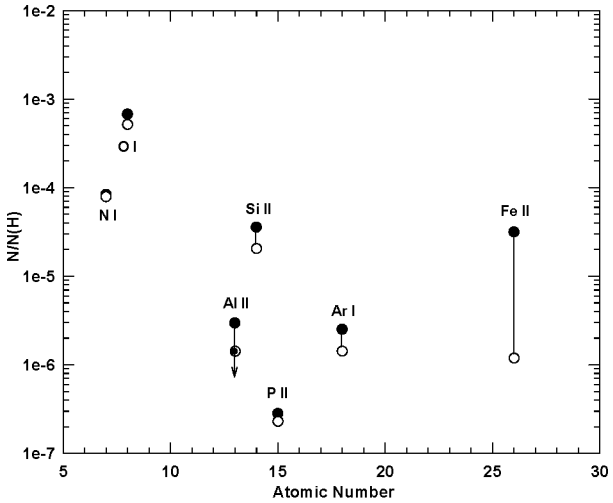

Fig. 4. Solar reference ion abundances normalized to hydrogen (Grevesse & Sauval 1998) are shown by filled circles while open circles are for the chemical composition of the ISM towards HR 5223.

5.1.1. Molecular and atomic hydrogen

The column density of neutral hydrogen has been deduced from the red wing of the interstellar Lβ line. In this way, the derived hydrogen CD gives a good agreement between observations and theory for the complete series of the hydrogen lines observed by FUSE (see Fig. 2), in particular for the Lα line detected by IUE (Fig. 3). Following the $N(\mathrm{H\ I})/E(B-V)$ relation derived by Shull & van Steenberg (1985), this CD corresponds to an ISM colour excess:

$$E(B-V) = 0.060 \pm 0.015 \text{ mag.} \quad (1)$$

We report in Fig. 4 the CD of the most abundant IS ions (open dots) and compare them to the solar abundances (Grevesse & Sauval 1998, filled circles). The plotted column densities are normalized to the total number, $N(\mathrm{H_{tot}})$, of hydrogen:

$$\begin{aligned} N(\mathrm{H_{tot}}) &= N(\mathrm{HI}) + 2\,N(\mathrm{H_2}) \\ &= 3.43 \pm 0.41 \times 10^{20}\ \mathrm{cm^{-2}}. \end{aligned} \quad (2)$$

This value is in good agreement with the results that can be obtained from H_2 indirectly using the statistical relations of Welty & Hobbs (2001, cf. Table 5).

5.1.2. The CNO elements

C II, N I and O I are the dominant ionization stages for CNO elements in the cold ISM. Concerning carbon, from 920 to 1180 Å no reliable C II line profile was available and the detected C I lines were very weak and blended. Consequently, it was only possible to set up an upper limit for the C I column density.

The nitrogen CD determination has been made using mostly the λ1134 N I multiplet lines and provides us the result N/H = (78.7 ± 13) × 10^{-6} which is very close to the mean value, N/H = (75 ± 4) × 10^{-6}, proposed by Meyer et al. (1997), but which is not significantly lower than the solar abundance, N/H = 83.2 × 10^{-6} reported by Grevesse & Sauval (1998). As expected the N depletion is about negligible.

Our determination of the interstellar oxygen abundance is mainly based on the study of the $\lambda\lambda$989 and 1039 O I line profiles. Following Cardelli et al. (1996) a depletion up to 180. × 10^{-6} relative to the Sun can be explained by dust formation. The O/H ratio, (516. ± 155.)× 10^{-6}, that we derived is 4/5 of the solar value proposed by Grevesse & Sauval (1998), which means a depletion of 160. × 10^{-6} and the observed ratio is 1.7 times greater than the average value, O/H = 319. × 10^{-6}, derived by Meyer et al. (1998) using GHRS data. The same authors found no significant dependence with the mean hydrogen density $n_{\mathrm{H}} = N(H_{\mathrm{tot}})/d_*$), where d_* is the distance to the observed star. However the STIS observations analyzed by Howk et al. (2000, see Fig. 2) show that at $n_{\mathrm{H}} < 0.30$ the O/H ratio is more scattered than at larger values. It is also worth noting that in a recent review paper Holweger (2001) determined, accounting for departures from LTE and solar granulation, an O/H = (545 ± 42) × 10^{-6} which is not significantly different from our result. If these results are confirmed, it implies that the ISM towards our star is not depleted in oxygen relative to the Sun.

5.1.3. Al II, Si II, P II, Cl I, Ar I and Fe II

We produce CDs for other elements such as Al, Si, P, Cl, Ar and Fe. If we except Cl I, which also exists in a single ionized form, all these ions represent the dominant ionization stage in the ISM (Savage & Sembach 1996).

The available and most visible Al II and Cl I lines (Al II λ935.28 Å and Cl I $\lambda\lambda$ 1004.68, 1031.51 Å) are strongly blended with molecular hydrogen lines and the respective ion abundances have to be taken carefully. At worse,

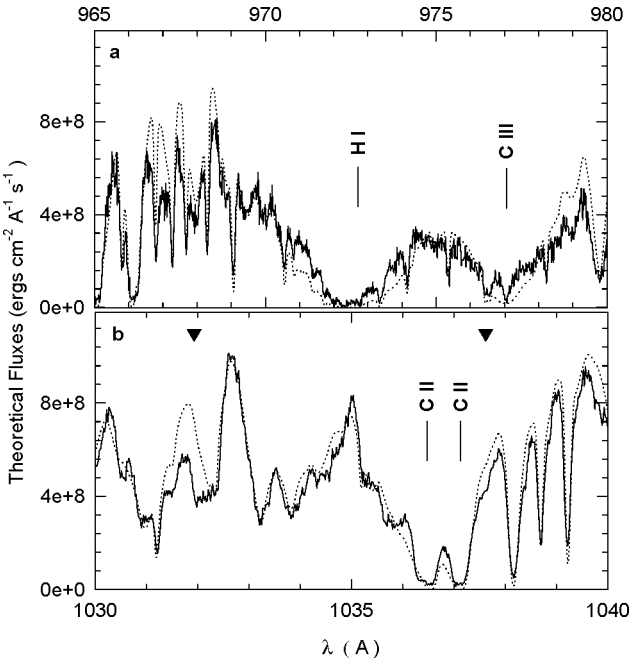

Fig. 5. Fits of observed spectra with theoretically predicted fluxes. In both panels the theoretical spectra (dotted lines) are computed assuming 0.7 dex lower carbon abundance than in the Sun. Observations are represented with a solid line, while the possible location of the O VI doublet is showed by plain triangles.

they could be considered as an upper limit. Si, P and Ar are found to be underabundant relative to the Solar abundance by −0.24, −0.09 and −0.29 dex respectively. Using observations from the Copernicus satellite, Jenkins et al. (1986) already found that phosphorus could be depleted by −0.17 dex while high resolution GHRS observations (Sembach & Savage 1996) and Interstellar Medium Absoption Profile Satellite observations (Sofia & Jenkins 1998) showed that the silicon and argon depletion may vary respectively from −0.35 to −0.51 and from −0.18 to −0.61. As expected for refractory species, Iron was also found to be depleted and follows the trend outlined by the recent GHRS observations (Wakker & Mathis 2000).

5.2. Stellar spectrum

221 transitions belonging to the photosphere were identified in the FUSE spectrum of HR 5223. Most elements are present in a single or doubly ionized form and the highest ionization level is reached by phosphorus (λ1030.5 P IV) and sulphur (λ1073 Si IV). No emission has been detected and generally there is a good agreement between theory and observations, if we exclude the spectral regions containing carbon lines, those perturbed by instrumental line features or those exhibiting airglow emission lines (mainly in the core of the hydrogen lines). Discrepancies due to carbon can be explained by an abundance 0.7 dex lower than in the Sun (Fig. 5). If we except this peculiar case, element abundances are close to the solar pattern.

In some active early B type stars, lines belonging to superionized atoms that should be produced by Auger ionization in the stellar wind (Owocki et al. 1988; Cassinelli & Olson 1979), and such as the λλ1032 and 1037 O VI doublet for the far-UV, have been detected (Lamers & Rogerson 1978). As our calculations do not account for this possible ionization process, the presence of the O VI doublet in the spectra of HR 5223 could be nevertheless identified if a disagreement between the observations and the computed spectrum appeared at 1032 Å and 1037 Å. Consequently, in order to test the possible presence of the O VI lines, and only once the peculiar carbon abundance in our star has been accounted for, we analyzed in detail the spectral range between 1030 and 1040 Å. As seen in Fig. 5, where observations are represented with a solid line and theory with a dotted line, at 1032 Å there is a clear disagreement between observations and theory. This disagreement could be attributed to the existence of an asymmetric line profile such as the one we could expect from the O VI lines. The same type of signature, though smaller, could also be expected in the second component of the doublet, but we find no visible trace of it at 1037 Å. This would imply that there is no O VI line at all in the spectrum. However, it is worth noting that the carbon abundance we estimated in order to reproduce the studied region can still be too high. In this case, the strong blends that we identified at these wavelengths might be possibly hiding an underlying λ1037 O VI small component. So, as the presence of the O VI doublet in the stellar spectrum of HR 5223 should not be excluded, a further more detailed analysis of this spectral region is needed to assert its presence.

6. Distance determination

6.1. Stellar fundamental parameters

We determined the fundamental parameters of the star by fitting the energy distribution between 920 and 3300 Å. Observations are from FUSE (920−1180 Å), IUE (1180−2200 Å) and ANS (2200−3300 Å), which were dereddened using the mean extinction curves proposed by Cardelli et al. (1989) and O'Donnell (1994). The theoretical fluxes take into account the effects of gravitational darkening due to the stellar fast rotation.

Four slightly different procedures were adopted to carry out the fits. In the first one (marked as $n = 1$ in Table 4) we studied the observed flux in the λλ 1700–3300 Å wavelength interval, normalized at 5555 Å. The normalization of the observed fluxes was done adopting the V magnitude corresponding to a phase of minimum line and continuum emission ($V = 6.25$ mag, Moujtahid et al. 1999), when the CE has no visible effect on the Balmer discontinuity. The same procedure was also used for the attempt $n = 2$, where the spectral range studied was λλ 920–3300 Å, which includes the FUSE far-UV spectral region. In $n = 3$ we used the same spectral range as in n = 1, but normalized at 3300 Å. Finally, in a fourth

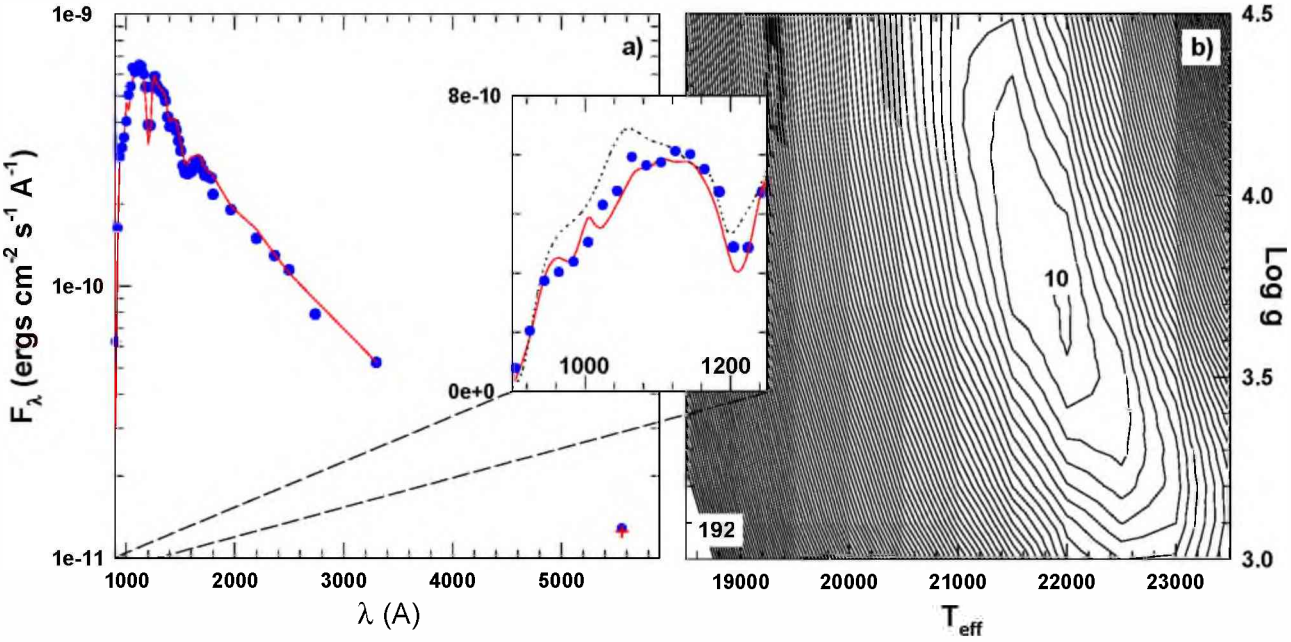

Fig. 6. a) Comparison at low resolution (50 Å) between observations (filled dots) and computed spectra with (solid line and cross) and without IS lines (dotted line). **b)** χ^2 minimization for the second fit procedure (curve of constant $\chi_2 = 192$ and $\chi_2 = 10$ are labeled).

Table 4. Fundamental parameters for HR 5223.

n	Range Å	$T_{\rm eff}$ K	log g $[g]$ = cgs	i deg.
1	1700 – 3300	20 500	*3.7*	*14*
2	920 – 3300	22 000	3.7	15
3	920 – 3300	23 500	3.9	14
4	920 – 3300	23 000	3.9	14

attempt ($n = 4$) we simply calculated monochromatic flux ratios $\mathcal{R}_\lambda = f_\lambda({\rm obs.})/F_\lambda({\rm model})$ in the $\lambda\lambda$ 920–3300 Å spectral region and sought for the $(T_{\rm eff}, \log g)$ parameters which produced the smallest dispersion of $\mathcal{R}_\lambda$ values.

The synthetic spectra were computed accounting for the effects of fast rotation, effective temperatures ranging from 16 000 K to 27 000 K by steps of 500 K and for log g varying from 3.0 dex to 4.5 dex by steps of 0.1 dex. The angular velocity, ω, of HR 5223 was taken to be $\omega = \Omega/\Omega_{\rm c} = 0.8$ (Chauville et al. 2001), where $\Omega_{\rm c}$ is the breakup velocity. The inclination angle i was determined using $V \sin i = 70$ km s^{-1} and the step by step $(T_{\rm eff}, \log g)$-dependent mass, luminosity and radius of the star at rest taken from the evolutionary tracks calculated by Schaller et al. (1992). We finally selected the best fit by using the χ^2 test (e.g. Fig. 6b). The final $(T_{\rm eff}, \log g)$ and inclination angle i adopted in each procedure are given in Table 4.

The fit carried out in $n = 1$ showed no clear dependence with $\log g$. We used in this case the wings of the Balmer hydrogen lines to determine the parameter log g. Differences in the $(T_{\rm eff}, \log g)$ determinations can be partially due to the fitting failures in the monochromatic fluxes used for normalizations, which determine the minimum χ^2 value. However, we also see that including the far-UV spectrum, which is generally formed in the upper layers of the photosphere, leads to a higher effective temperature. This suggests that the temperature in the outermost layers may perhaps be somewhat hotter than predicted in Kurucz' radiative equilibrium model atmospheres. It should not also be excluded that energy release due to hydrodynamic instabilities produced by the fast rotation and/or back radiation from the CE (Hoeflich 1988) could be the cause of this heating that increases the uncertainty on the fundamental parameters of HR 5223. We finally adopted the $(T_{\rm eff}, \log g)$ estimate which not only produced the lowest value of χ^2, but also better represented the flux in the V magnitude at the stellar minimum emission phase. Thus, the parameters we have obtained for a HR 5223 homologous rotationless star, are:

$$\left.\begin{array}{lll} T_{\rm eff} & = & 22\,000 \text{ K} \\ \log\ g & = & 3.7 \\ i & = & 15^\circ \end{array}\right\}. \qquad (3)$$

Finally, it is also worth noting that the effects of gravitational darkening due to fast rotation are more important in the far-UV, where the flux can be overestimated if these effects are not taken into account. In the case of a pole-on B2 III object seen at 1000 Å, our computations show that for $\omega = 0.8$ the flux of the rotating star is 13% greater than what is expected from a normal Kurucz model with the same $(T_{\rm eff}, \log g)$ parameters.

6.2. Distance

HR 5223 has been observed with the HIPPARCOS satellite, but the telescope could not resolve its parallax ($\pi_{\rm HIP} = 0.00 \pm 0.84$ mas). If we define the horizon of the

HIPPARCOS satellite as the distance above which each star observed has a relative parallax error greater or equal to 100%, then HR 5223 is probably located close or beyond this limit. To estimate the stellar distance, we used then the theoretical fluxes in the $\lambda\lambda$ 920–3300 Å wavelength interval for the adopted fundamental parameters. We calculated the average angular diameter:

$$\theta = \overline{\left(\frac{4}{\pi}\frac{f_\lambda}{F_\lambda(\omega,i)}\right)^{1/2}} = \frac{2R_\circ}{d}\frac{R_e(\omega)}{R_\circ} \quad (4)$$

where f_λ are the observed and dereddened stellar fluxes, F_λ are the theoretically predicted astrophysical fluxes emitted by the observed stellar hemisphere, d is the distance of the star, $R_\circ$ is the stellar radius if the star had no rotation and $R_e(\omega)$ is the equatorial radius of the star at the rotational rate ω. For $\omega = 0.8$ we have $R_e/R_\circ = 1.132$. Using the tables of Schaller et al. (1992) for the adopted $(T_{\rm eff}, \log g)$ parameters we have:

$$\log\ L(\omega=0)/L_\odot = 4.066, M/M_\odot = 10.0, R_\circ/R_\odot = 7.42.$$

Thus from relations (4) we derive:

$$d = 834 \pm 20\,\mathrm{pc}. \quad (5)$$

We note that for the distance obtained using the monochromatic observed and predicted fluxes at λ5555 Å we obtain d = 829 pc. On the other hand, calculating the bolometric flux of the HR 5223 from the measured ones in the $\lambda\lambda$ 920–8000 Å and completed in the remaining wavelength intervals using model atmospheres (only 1.3% of the observed ones), as well as the theoretically predicted bolometric luminosity for the observed hemisphere, $\log L(\omega,i)/L_\odot = 4.145$, we derive d = 842 pc. Both estimates of d are within the 2.4% uncertainty limits of the distance determination from the far-UV fluxes.

We also point out that the distance obtained is much greater than the value given by the statistical relation proposed by Shull & van Steenberg (1985):

$$< d_* >= \frac{< N(\mathrm{HI}) >}{0.46} \times 3.24076 \times 10^{-19} = 220\ \mathrm{pc}. \quad (6)$$

The discrepancy can be explained by the fact that the relation given by Shull & van Steenberg (1985) does not account for the irregular distribution of the ISM absorbing matter. This can be readily seen by plotting the $E(B-V)$ colour excess against the distance of a sample of stars within 5 degrees around HR 5223. In Fig. 7, distances were derived from HIPPARCOS trigonometric parallaxes, while colour excesses were computed comparing measured $(B-V)$ colour indices to the respective spectral type intrinsic values. An increase of the reddening clearly occurs from 0 to 250 parsecs with a regular slope of about 0.5 mag kpc^{-1} confirmed by Lucke (1978, see Fig. 9 and Fig. 10). This $E(B-V)$ increase can be attributed to the Lower Centaurus Crux (LCC) loop which is located at 140 parsecs from the Sun (de Geus 1992) and has a mean radius of about 45 parsecs (Crawford 1991). Beyond this gradient, from 250 pc to 900 pc, where another IS cloud is detected, the colour excess remains near constant. So, the distance derived from Eq. (6) has to be seen as a lower value corresponding to the outermost limit of the LCC. This finally locates HR 5223 very close to HIPPARCOS' horizon (Fig. 7) above which there exist no reliable parallax determination.

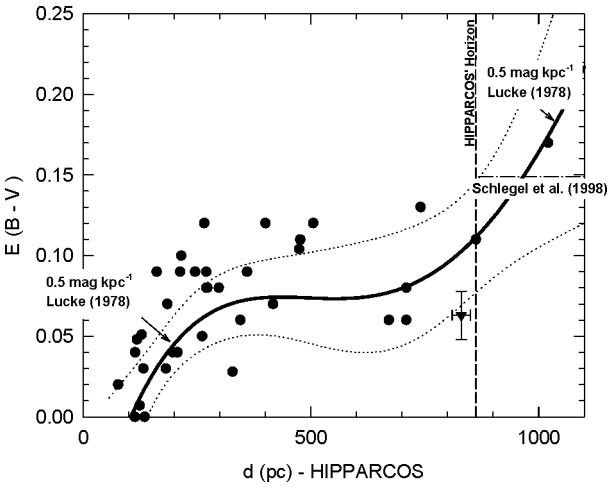

Fig. 7. Colour excess versus distance for a sample of stars within 5 degrees around HR 5223 (triangle). Galactic reddening in the same direction is represented by a dashed-dotted line (Schlegel et al. 1998). $E(B-V)$ gradients proposed by Lucke (1978) for the studied region are labeled on the same figure. Dotted lines represent the confidence level on the polynomial fit (solid line).

7. Final discussion and conclusion

Far-UV data obtained by FUSE for the pole-on Be star HR 5223 allowed us to determine the column densities of several elements which appear in the ISM. Most of the studied elements are depleted relative to the solar abundance in the same way that they are in other lines of sight.

The presence of the interstellar lines sensitively lowers the global energy distribution in the far-UV (Fig. 6). Once accounting for this effect, neither continuum emission nor line emission, even in the first hydrogen lines of the Lyman series were observed in the FUSE spectra. In particular, in the FUSE wavelength range we found no trace of any spectral characteristic that could be attributed to the circumstellar envelope. As shown by the good agreement we found between observations and theory, the total hydrogen column density enabled us to determine a reliable value of the $E(B-V)$ colour excess towards HR 5223 due only to the ISM.

The column densities of the IS elements observed towards the star clearly show that HR 5223 is located between 250 pc and 900 pc. The distance of the star was determined from a direct comparison of the UV observations to theoretical spectra that accounted for effects of fast rotation.

The characteristics of the O VI resonance lines in the FUSE spectral region and the circumstances of its

appearance, together with those of C IV and Si IV resonance lines seen in the IUE spectra, will be discussed in a separate contribution.

Acknowledgements. We would like to thank Drs M. Lemoine, I. Hubeny and T. Lanz for allowing us to use their computer codes. We thank Dr A. Lecavelier des Etangs for his comments and help in using the OWENS computer code. We also wish to thank Dr B.D. Savage, our referee, for useful comments that improved the final version of our paper.
This research has been partially supported by a Marie Curie Fellowship of the European Community programme FP5 under contract number HPMF-CT-2000-00497.
Our work is based on INES data from the IUE and FUSE satellites while bibliographic researches were perform using the SIMBAD and ADS databases.

References

Campbell, W. W. 1895, ApJ, 2, 177
Cardelli, J. A., Clayton, G. C., & Mathis, J. S. 1989, ApJ, 345, 245
Cardelli, J. A., Meyer, D. M., Jura, M., & Savage, B. D. 1996, ApJ, 467, 334
Cassinelli, J. P., & Olson, G. L. 1979, ApJ, 229, 304
Chauville, J., Zorec, J., Ballereau, D., et al. 2001, A&A, 378, 861
Crawford, I. A. 1991, A&A, 247, 183
Dachs, J., & Hanuschik, R. 1984, A&A, 138, 140
Dachs, J., Hummel, W., & Hanuschik, R. W. 1992, A&AS, 95, 437
de Geus, E. J. 1992, A&A, 262, 258
Feldman, P. D., Sahnow, D. J., Kruk, J. W., Murphy, E. M., & Moos, H. W. 2001, J. Geophys. Res., 106, 8119
Fleming, M. 1890, Astron. Nachr., 125, 363
Grevesse, N., & Sauval, A. J. 1998, Space Science Reviews, 85, 161
Hanuschik, R. W. 1996, A&A, 308, 170
Hanuschik, R. W., Hummel, W., Dietle, O., & Sutorius, E. 1995, A&A, 300, 163
Hanuschik, R. W., Hummel, W., Sutorius, E., Dietle, O., & Thimm, G. 1996, A&AS, 116, 309
Hiltner, W. A., Garrison, R. F., & Schild, R. E. 1969, ApJ, 157, 313
Hoeflich, P. 1988, A&A, 191, 348
Holweger, H. 2001, in Joint SOHO/ACE workshop Solar and Galactic Composition, ed. (R. F. Wimmer-Schweingruber), (Publisher: American Institute of Physics), Conf. Proc., 598, 23
Howk, J. C., Sembach, K. R., & Savage, B. D. 2000, ApJ, 543, 278
Hubeny, I. 1988, Comput. Phys. Commun., 2, 103
Hubeny, I., Harmanec, P., & Stefl, S. 1986, Bulletin of the Astronomical Institutes of Czechoslovakia, 37, 370
Hummel, W. 1994, A&A, 289, 458
Jaschek, M., Slettebak, A., & Jaschek, C. 1981, Be Stars Newsletter, 4, 19
Jenkins, E. B., Savage, B. D., & Spitzer, L. 1986, ApJ, 301, 355
Kurucz, R. L. 1994, SAO CDROM N19
Lamers, H. J. G. L. M., & Rogerson, J. B. 1978, A&A, 66, 417
Lemoine, M., Audouze, J., Ben Jaffel, L., et al. 1999, New Astronomy, 4, 231
Lucke, P. B. 1978, A&A, 64, 367
Meyer, D. M., Cardelli, J. A., & Sofia, U. J. 1997, ApJ, 490, L103
Meyer, D. M., Jura, M., & Cardelli, J. A. 1998, ApJ, 493, 222
Moos, H. W., Cash, W. C., Cowie, L. L., et al. 2000, ApJ, 538, L1
Morton, D. C. 2001, Private communication
Moujtahid, A., Zorec, J., & Hubert, A. M. 1999, A&A, 349, 151
O'Donnell, J. E. 1994, ApJ, 422, 158
Owocki, S. P., Castor, J. I., & Rybicki, G. B. 1988, ApJ, 335, 914
Sahnow, D. J., Moos, H. W., Ake, T. B., et al. 2000, ApJ, 538, L7
Savage, B. D., & Sembach, K. R. 1996, ARA&A, 34, 279
Schaller, G., Schaerer, D., Meynet, G., & Maeder, A. 1992, A&AS, 96, 269
Schlegel, D. J., Finkbeiner, D. P., & Davis, M. 1998, ApJ, 500, 525
Sembach, K. R., & Savage, B. D. 1996, ApJ, 457, 211+
Shull, J. M., & van Steenberg, M. E. 1985, ApJ, 294, 599
Slettebak, A. 1982, ApJS, 50, 55
Sofia, U. J., & Jenkins, E. B. 1998, ApJ, 499, 951+
Wakker, B. P., & Mathis, J. S. 2000, ApJ, 544, L107
Welty, D. E., & Hobbs, L. M. 2001, ApJS, 133, 345